Glacio-isostatic adjustment in Fennoscandia revisited

Detlef Wolf*

Department of Physics, University of Toronto, Toronto, Ontario, Canada, M5S 1A7

Abstract. The theory of load-induced relaxation of the layered Maxwell half-space is applied to the study of glacio-isostatic adjustment in Fennoscandia. The interpretation uses emergence data from Ångermanland (Sweden) and uplift-rate data from the Gulf of Bothnia. With mantle viscosity fixed at 10^{21} Pa s, the data can be explained by an earth model characterized by (a) an elastic surface layer of conventional thickness (about 100 km) superimposed on a low-viscosity layer or (b) an elastic surface layer of enhanced thickness (about 200 km) and no low-viscosity layer. Reasons for this ambiguity and possible ways to resolve it in future studies are suggested. The investigation also attempts to interpret the negative free-air gravity anomaly observed over the deglaciated region of Fennoscandia. Either (i) enhanced mantle viscosity below 670 km depth or (ii) a transition zone in viscosity between an elastic surface layer and a viscous mantle is required to predict negative anomalies substantially larger than 3 mgal.

Key words: Fennoscandia – Isostasy – Maxwell continuum

Introduction

More than 50 years ago, Reginald Daly drew attention to post-glacial uplift and discussed two rheological earth models, which he designated "bulge hypothesis" and "punching hypothesis" (Daly, 1934, pp. 120–126).

The bulge hypothesis assumes that flow is restricted to a near-surface layer (channel model). Mass conservation then requires the existence of a substantial peripheral bulge during glaciation. During and after deglaciation, the central depression is elevated to equilibrium while the bulge collapses.

Daly believed that geological evidence in support of a peripheral bulge is missing in Fennoscandia and North America. He therefore suggested that the glacial load had been punched through the elastic crust, forcing flow to great depths (deep-flow model). A distinctive feature of this model is that, with deglaciation, both central and peripheral regions are initially uplifted sympathetically. The later stages of readjustment include crustal failure and a reversal of the upward movement in the periphery (Daly, 1934, Fig. 70).

The following year, Haskell (1935) demonstrated quantitatively that the main features of Daly's punching hypothesis are also produced by a uniform, Newtonian viscous half-space. Haskell also interpreted the Fennoscandian uplift with this model. His estimate of the dynamic mantle viscosity was about 10^{21} Pa s. An essential ingredient of Haskell's analysis was the assumption of a residual depression of 20 m near the glaciation centre, corresponding to a free-air gravity anomaly of approximately -3 mgal.

The question of the causal relation between the observed gravity anomaly and the Pleistocene glaciation in Fennoscandia has been discussed since Haskell's pioneer study (summarized by Cathles, 1975, pp. 151–154; Balling, 1980). The difficulties in interpreting the gravity field are related to the fact that, although negative anomalies predominate in Fennoscandia, the gravity pattern is irregular. In particular, there is no pronounced correlation with the topography of the Pleistocene ice-sheet. Therefore, differing values for the remaining uplift can be inferred from the free-air gravity data.

Niskanen (1939), for example, suggested that the deglaciation-induced portion has a peak value of about -30 mgal, giving a residual depression of about 200 m. This led several investigators to dismiss Haskell's deep-flow model and use various kinds of channel model, which produce enhanced residual depressions. The quantitative development of channel models was initiated by van Bemmelen and Berlage (1935) and subsequently extended by many other investigators (summarized by Cathles, 1980; Walcott, 1980). Since there is now evidence for an almost uniformly viscous mantle (Cathles, 1975; Peltier and Andrews, 1976; Wu and Peltier, 1983), channel models have fallen into disrepute.

Recently, Balling (1980) attempted to substantiate previous claims of more moderate deglaciation-induced anomalies (e.g. Walcott, 1973). After filtering out a non-glacial component believed to be related to the structure of the earth's crust and upper mantle, Balling inferred a glacial component of about -17 mgal for central Fennoscandia (Fig. 1). This value implies that the positive anomalies in the peripheral region reflect a superimposed long-wavelength geoid high. However, deglaciation-induced anomalies of this order are still substantial and, as Haskell's (1935) and Cathles' (1975) work shows, incompatible with simple deep-flow models.

A possible way out of this impasse was proposed by Anderson (1984). Using statistical analysis, he suggested
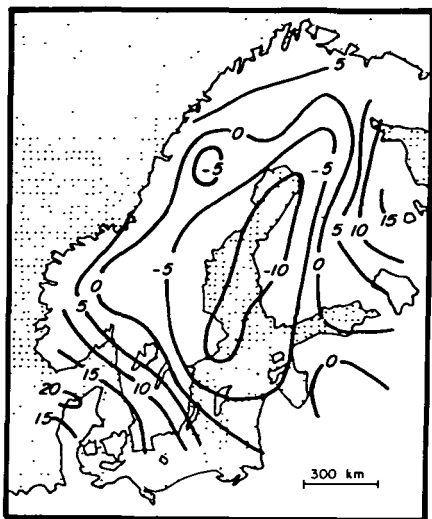
Fig. 1. Glacial component of free-air gravity anomaly in Fennoscandia (in units of mgal; after Balling, 1980)

that the observed geoid low over Fennoscandia is caused predominantly by an approximately twofold increase in crustal thickness from the Norwegian Sea and northern Germany toward central Fennoscandia. Anderson therefore concluded that contributions to the geoid anomaly associated with crustal structure are much more substantial than generally assumed. If this is true, the glacial component of the gravity anomaly must be quite small and can be easily explained with simple deep-flow models.

An alternative way to reconcile gravity observations with gravity predictions was discussed by Peltier and Wu (1982). Using Maxwell earth models, of essentially uniform viscosity and with the same density and elastic structure as seismic earth model 1066B (Gilbert and Dziewonski, 1975), Peltier and Wu predicted free-air gravity anomalies of about −20 mgal for Fennoscandia. The increase in magnitude was largely a consequence of treating the entire density structure of model 1066B as non-adiabatic.

It has also been suggested that an elastic surface layer

(lithosphere) is actively involved in the isostatic adjustment process in Fennoscandia. One of the modern investigators who devoted explicit attention to the lithosphere was McConnell (1968), who interpreted relaxation-time estimates from a spectral decomposition of strandline data from Fennoscandia. He used a layered, Newtonian viscous half-space model and proposed a lithospheric thickness of 120 km.

Cathles' study of glacio-isostatic adjustment was biased by his idea that the Fennoscandian uplift is insensitive to the presence of the lithosphere (Cathles, 1975, p. 153). In his flat-earth analysis, he arbitarily adopted a lithosphere of about 70 km thickness (Cathles, 1975, pp. 184–191). Recent results (Wolf, 1984, 1985a) showed that this is probably a misconception.

In the light of these inconsistencies, the present study re-interprets glacio-isostatic adjustment in Fennoscandia, based on the theory of the layered, incompressible Maxwell halfspace. The complex Fennoscandian deglaciation history is simulated by several simplified models. Particular attention is paid to the question of lithospheric thickness. The results will show that, although the adjustment data used are compatible with a lithosphere of about 200 km thickness below Fennoscandia, the data *cannot* be construed to require this value.

Further, the seismic discontinuity at 670 km depth is discussed in relation to the free-air gravity anomaly over Fennoscandia. According to the preliminary reference earth model (PREM; Dziewonski and Anderson, 1981), this discontinuity is characterized by a density increase of 390 kg m^{-3}, which is treated as non-adiabatic in the present study. Although the gravity predictions are largely insensitive to this density contrast, results will show that they are very sensitive to the value adopted for the viscosity below 670 km depth. The study also proposes an alternative explanation of the gravity anomaly, suggesting that it is related to the relaxation of a transition zone in viscosity between the elastic surface layer and the mantle.

Theoretical model

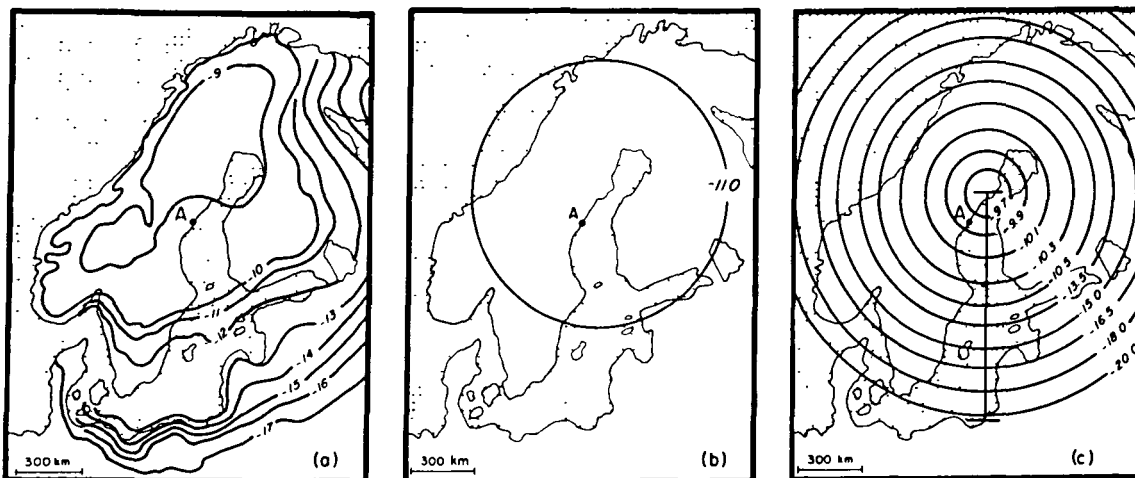The rheological model basic to this interpretation is the layered, incompressible Maxwell half-space. Each of its

Fig. 2a–c. a Fennoscandian deglaciation isochrons (after De Geer, 1954), **b** load model 1 and **c** load model 2: *A* denotes Ångermanland, *the bar* in **c** illustrates uplift-rate profile, times (in units of ka) are with respect to present time

Table 1. Parameters of load models

Cycle N	t (ka)		R (km)
Load model 1			
	$-\infty$ to	-11.0	600
	-11.0 to	0.0	0
Load model 2			
1	-2000.0 to	-1900.0	R
2	-1900.0 to	-1800.0	R
.	.	.	.
.	.	.	.
.	.	.	.
19	-200.0 to	-100.0	R
	-100.0 to	-80.0	200
	-80.0 to	-60.0	400
	-60.0 to	-40.0	600
	-40.0 to	-20.0	800
	-20.0 to	-18.0	1000
	-18.0 to	-16.5	900
	-16.5 to	-15.0	800
20	-15.0 to	-13.5	700
	-13.5 to	-10.5	600
	-10.5 to	-10.3	500
	-10.3 to	-10.1	400
	-10.1 to	-9.9	300
	-9.9 to	-9.7	200
	-9.7 to	-9.5	100
	-9.5 to	0.0	0

Table 2. Parameters of earth models

Layer l	h_l (km)	ρ_l (kg m^{-3})	μ_l (N m^{-2})	η_l (Pa s)
Earth model A.1				
1	100.0	3380	0.67×10^{11}	∞
2	100.0	3380	1.45×10^{11}	η_2
3	∞	3380	1.45×10^{11}	1.0×10^{21}
Earth model L.1				
1	h_1	3380	0.67×10^{11}	∞
2	∞	3380	1.45×10^{11}	1.0×10^{21}
Earth model L.4				
1	142.0	3380	0.67×10^{11}	∞
2	19.5	3380	0.67×10^{11}	1.0×10^{25}
3	24.1	3380	0.67×10^{11}	1.0×10^{23}
4	∞	3380	1.45×10^{11}	1.0×10^{21}
Earth model L.5				
1	93.7	3380	0.67×10^{11}	∞
2	28.7	3380	0.67×10^{11}	1.0×10^{25}
3	44.6	3380	0.67×10^{11}	1.0×10^{23}
4	∞	3380	1.45×10^{11}	1.0×10^{21}
Earth model M.4				
1	h_1	3380	0.67×10^{11}	∞
2	$670.0-h_1$	3380	1.45×10^{11}	1.0×10^{21}
3	∞	ρ_3	1.45×10^{11}	η_3

layers is characterized by four parameters: thickness h, density ρ, rigidity μ and viscosity η. The response of this model to surface loads was analysed and discussed previously (Wolf, 1985a).

The glaciation of Fennoscandia (Fig. 2a) is modelled as a Heaviside unloading event at 11 ka B.P. (Fig. 2b, Table 1, load model 1) and as a stepwise-discontinuous loading history (Fig. 2c, Table 1, load model 2). Load model 1 is the first approximation. It simulates the fast decay of the Fennoscandian ice-sheet following a period of stagnation between 12 and 10 ka B.P. Load model 2 is more realistic, although several important features of the Fennoscandian glaciation are unknown, for example, the extent of the ice-sheet in the shelf regions of the Norwegian and Barents Seas. However, the location of the uplift site employed in this study in Ångermanland (Sweden) (Fig. 2) is very close to the Pleistocene glaciation centre and therefore largely insensitive to complications near the ice margin.

Load model 1 can only be used with earth models that have short relaxation times (Table 2, earth models A.1 and L.1). For simplicity, the cross-section of load model 1 is assumed to be rectangular and the load thickness to be a free parameter. For the same earth models, load cycle 20 of load model 2 may also be used. This cycle uses a parabolic cross-section and a fixed ratio h_0^2/R between the square of axial load thickness h_0 and load radius R (details in Paterson, 1981, pp. 154–155; Wolf, 1985b). However, with earth models that support modes of long relaxation times (Table 2, earth models L.4, L.5 and M.4), the long-term glaciation history can no longer be neglected [see Imbrie and Imbrie (1979, pp. 153–173) on the time sequence of glaciations during the Pleistocene]. This is taken into account by load model 2, where load cycle 20 is preceded by 19 similar load cycles. For computational ease, the cross-section of the load is assumed to be rectangular and the load radius to be fixed during load cycles 1–19. During each of these cycles the load thickness increases according to $h_0(t-t_N)/(t_{N+1}-t_N)$, where t_N is the beginning of the N-th load cycle and $t_N < t < t_{N+1}$. The maximum thickness h_0 reached at the end of each cycle is determined by the ratio h_0^2/R adopted for load cycle 20. The load density is always assumed to be 1000 kg m^{-3}.

Data analysis and discussion

The emergence data from Ångermanland are of prime importance to this interpretation. The data set is based on a series of raised beaches, whose ages are constrained by varve sequences. The data were originally published by Lidén (1938), but can also be found elsewhere (e.g. Lliboutry, 1971; Cathles, 1975, p. 196). Since the dating of the strandlines is based on varve chronology, the relative ages of the Ångermanland strandline series are very accurate.

The observed emergence of a strandline is controlled by uplift of the earth's surface *and* by changes in sea level. Sea-level changes are related to (a) influx of melted ice and (b) geoid perturbations produced by redistribution of water and by simultaneous redistribution of mantle material. Contribution (a) has been named eustatic change. This has a clear meaning only if it is defined as the ocean-wide average change in mean sea level (Walcott, 1972). Contribution (b) depends on location but can become as large as contribution (a) (Farrell and Clark, 1976; Clark et al., 1978; Peltier et al., 1978).

Near major glaciation centres, sea-level changes have been small compared with surface uplift after about 10 ka B.P. Before that, the lowering of eustatic sea level was partially counterbalanced by the rise of the geoid below the melting ice mass (Wu and Peltier, 1983, Fig. 4a). The portion of the emergence of old strandlines caused by uplift

of the earth's surface may therefore be approximately bracketed by the observed emergence and this emergence corrected for eustatic sea-level rise.

The following uplift diagrams symbolize this range by vertical bars, where corrections for eustatic sea-level change according to Fairbridge (1961, Fig. 8) have been applied. The observed uplift during the time interval $[t,0]$ can now be compared with the predicted uplift $H(t) = w(t) - w(0)$, where w is the (downward) surface displacement for the model under consideration and $t = 0$ is present time.

The study of the Fennoscandian uplift begins by using load model 1. The observed uplift in Ångermanland is compared with the theoretical uplift for two distinct earth models, both of which use a mantle viscosity of 10^{21} Pa s.

Figure 3a shows an interpretation similar to that proposed by Cathles (1975, pp. 184-191), with a load thickness of 1.50 km. The earth model uses a lithosphere of *conventional* thickness (100 km) underlain by a low-viscosity layer (asthenosphere) (Table 2, earth model A.1). If the viscosity of the asthenosphere is selected properly, a satisfactory fit of the data is achieved.

Figure 3b proposes an alternative interpretation of the same data set. The load thickness has been increased to 1.90 km, and the Earth model has a lithosphere but no asthenosphere (Table 2, earth model L.1). This time the data are bracketed by the curves for *enhanced* lithospheric thicknesses of 170 km and 230 km.

If the load thickness is further increased, the observations are compatible with even larger lithospheric thicknesses. Conversely, the fit produced in Fig. 3a is a consequence of the reduced load thickness that is used. This behaviour is consistent with results by Wolf (1985a, Figs. 10a and 11a). The ambiguous interpretation is therefore partly a consequence of a trade-off between lithospheric thickness and load thickness.

The next step is to use earth model L.1 with load model 2. For lithospheric thicknesses of about 200 km, this requires $h_0^2/R = 4.0 \times 10^{-3}$ km. As Fig. 4a shows, the fit of the uplift data is similar to that in Fig. 3b. Closer inspection of Fig. 4a reveals, however, that younger beaches are consistent with a lithosphere slightly thinner than 200 km, whereas older beaches are better explained if the lithosphere is somewhat thicker.

Figure 4b shows the observed uplift rates (e.g. Balling, 1980) on a north-south profile in the Gulf of Bothnia (Fig. 2c) as stippled band and the theoretical uplift rates for the same model parameters. The uplift rates are obviously very sensitive to lithospheric thickness. Similarly to Fig. 4a, a thickness of approximately 170 km produces the best fit.

As expected, the theoretical models discussed so far have small free-air gravity anomalies. For the 200 km thick lithosphere, the peak value is approximately -4 mgal, giving a residual depression of about 28 m. If Balling's (1980) filtered anomaly (Fig. 1) represents the deglaciation-induced portion of the gravity field in Fennoscandia, this interpretation appears untenable.

The study therefore investigates the effects of a contrast in viscosity or density at 670 km depth (Table 2, earth model M.4). The modifications apply to a saw-tooth loading history (Fig. 5) and are shown in Fig. 6. The radius of 1000 km for the rectangular load is selected to represent conditions during the last glacial maximum at about 18 ka B.P. The sensitivity of the response to lower-mantle viscosity
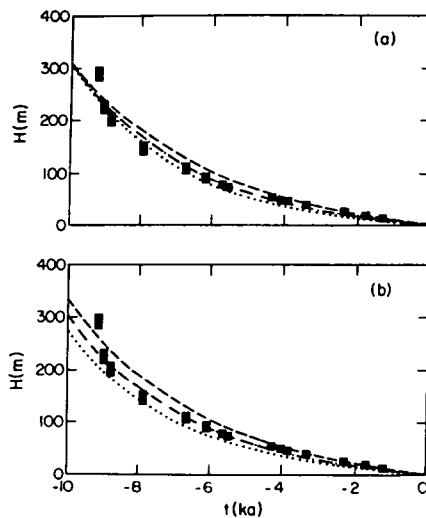

Fig. 3a and b. Ångermanland uplift data (Lidén, 1938) and uplift prediction H as functions of time t; **a** applies to load model 1 with $h_0 = 1.50$ km and earth model A.1 with $\eta_2 = 5.0 \times 10^{19}$ Pa s (*dashed*), $\eta_2 = 1.5 \times 10^{19}$ Pa s (*dot-dashed*) or $\eta_2 = 1.0 \times 10^{19}$ Pa s (*dotted*); associated free-air gravity prediction at $r = 0$, $t = 0$ is $\Delta g = -6.1$ mgal (*dashed*), $\Delta g = -3.4$ mgal (*dot-dashed*) or $\Delta g = -2.4$ mgal (*dotted*); **b** applies to load model 1 with $h_0 = 1.90$ km and earth model L.1 with $h_1 = 170$ km (*dashed*), $h_1 = 200$ km (*dot-dashed*) or $h_1 = 230$ km (*dotted*); associated free-air gravity prediction at $r = 0$, $t = 0$ is $\Delta g = -5.7$ mgal (*dashed*), $\Delta g = -3.9$ mgal (*dot-dashed*) or $\Delta g = -2.7$ mgal (*dotted*)
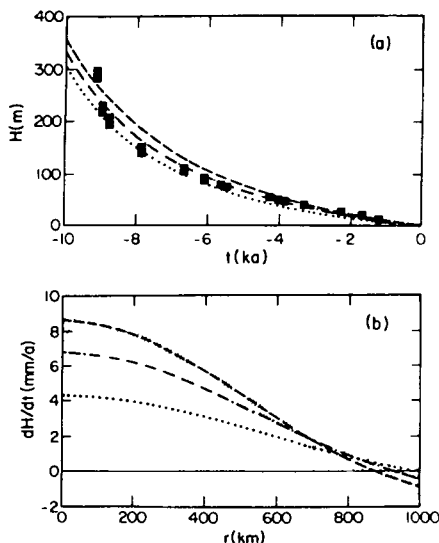

Fig. 4a and b. a Ångermanland uplift data (Lidén, 1938) and uplift prediction H as functions of time t and **b** Gulf of Bothnia uplift-rate data (Balling, 1980) and uplift-rate prediction dH/dt as functions of axial distance r; predictions apply to load model 2 with $h_0^2/R = 4.0 \times 10^{-3}$ km and earth model L.1 with $h_1 = 170$ km (*dashed*), $h_1 = 200$ km (*dot-dashed*) or $h_1 = 230$ km (*dotted*); associated free-air gravity prediction at $r = 0$, $t = 0$ is $\Delta g = -5.6$ mgal (*dashed*), $\Delta g = -4.0$ mgal (*dot-dashed*) or $\Delta g = -2.8$ mgal (*dotted*)

is obvious. At time $t = 12$ ka, the residual surface depression is increased threefold for a twofold increase in lower-mantle viscosity. The modifications produced by the internal density contrast are much smaller in comparison.

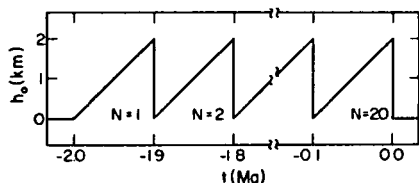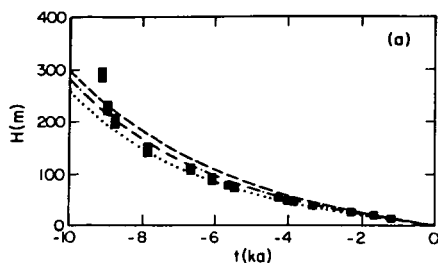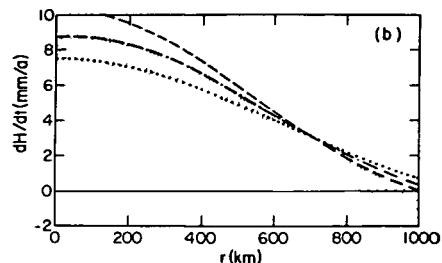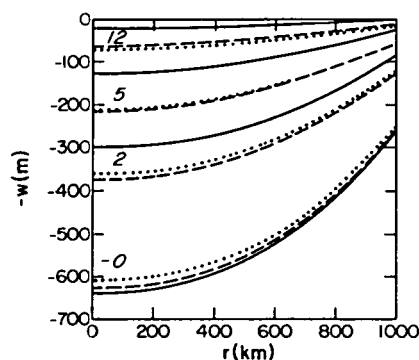Figure 7 interprets the Ångermanland uplift data using
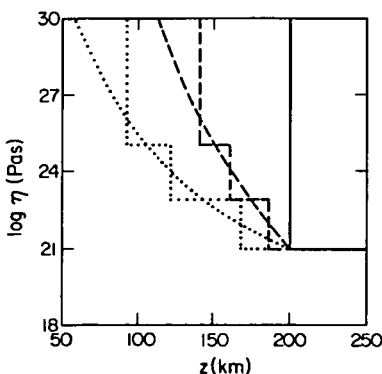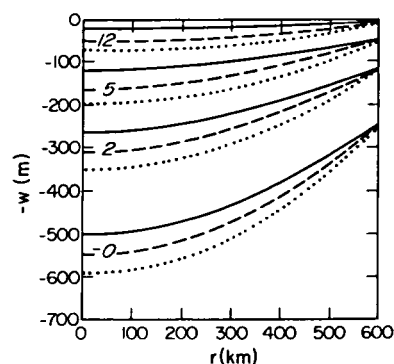
Fig. 5

Fig. 7a

b

Fig. 6

Fig. 8

Fig. 9

Fig. 5. Saw-tooth loading history applicable to Figs. 6, 9 and 11

Fig. 6. Vertical surface displacement w as function of axial distance r for several times (in units of ka) after load removal; predictions apply to saw-tooth loading history (Fig. 5) with R = 1000 km and earth model M.4 with $h_1 = 200$ km and $\rho_3-\rho_2 = 0$, $\eta_3 = 1.0 \times 10^{21}$ Pa s (*solid*), $\rho_3-\rho_2 = 0$, $\eta_3 = 2.0 \times 10^{21}$ Pa s (*dashed*) or $\rho_3-\rho_2 = 390$ kg m^{-3}, $\eta_3 = 2.0 \times 10^{21}$ Pa s (*dotted*)

Fig. 7a and b. As for Fig. 4 except that predictions apply to load model 2 with $h_0^2/R = 3.0 \times 10^{-3}$ km and earth model M.4 with $\rho_3-\rho_2 = 390$ kg m^{-3}, $\eta_3 = 2.0 \times 10^{21}$ Pa s and $h_1 = 170$ km (*dashed*), $h_1 = 200$ km (*dot-dashed*) or $h_1 = 230$ km (*dotted*); associated free-air gravity prediction at $r = 0$, $t = 0$ is $\Delta g = -9.4$ mgal (*dashed*), $\Delta g = -7.7$ mgal (*dot-dashed*) or $\Delta g = -6.4$ mgal (*dotted*)

Fig. 8. Viscosity η as function of depth z for $Q \rightarrow \infty$ (*solid*), $Q = 500$ kJ mol^{-1} (*dashed*) or $Q = 200$ kJ mol^{-1} (*dotted*); continuous functions are approximated by three uniform layers

Fig. 9. As for Fig. 6 except that predictions apply to saw-tooth loading history (Fig. 5) with R = 600 km and earth model L.1 with $h_1 = 200$ km (*solid*), earth model L.4 (*dashed*) or earth model L.5 (*dotted*)

this earth model. Compared with the model used for Fig. 4, the viscosity below 670 km is higher by a factor of two and the density is increased by 390 kg m^{-3} in this depth range. As before, results apply to load model 2. During load cycles 1–19, $R = 1000$ km; during load cycle 20, $h_0^2/R = 3.0 \times 10^{-3}$ km. The reduction in load thickness, compared with Fig. 4, is required to predict the correct present-day uplift rates. The fit of the uplift and uplift-rate data is comparable to Fig. 4, but the theoretical free-air gravity anomaly is enhanced significantly ($\Delta g = -7.7$ mgal for $h_1 = 200$ km).

In order to predict a value near -17 mgal, either additional internal buoyancy or a further increase in lower-mantle viscosity is required. Neither alternative appears practicable, however. Whereas the former hinges on the assumption that each additional density discontinuity is modelled as a non-adiabatic increase, the latter renders a satisfactory fit of the uplift and uplift-rate data increasingly difficult.

An alternative mechanism for enhancing gravity predictions is provided by the introduction of a transition zone

in viscosity between the elastic surface layer and the viscous mantle. For example, assuming a linear geotherm which passes through points $T = 0°$ C, $z = 0$ km and $T = 1400°$ C, $z = 200$ km (Jordan, 1981), the temperature distribution can be converted into a viscosity distribution, provided that the viscosity η at depth $z = 200$ km and the activation energy Q in the depth range $0 \leq z \leq 200$ km are known (details in Wolf, 1985a).

Figure 8 uses a mantle viscosity of 10^{21} Pa s and shows viscosity-depth distributions for three activation energies. For computational ease, the continuous distributions are approximated by three uniform layers, which constitute the *thermal* lithosphere (Table 2, earth models L.4 and L.5). The portion which responds elastically is called the *mechanical* lithosphere. If the loading time is sufficiently short or if the activation energy is sufficiently high, the "mechanical thickness" approaches the "thermal thickness".

The modifications of the response produced by a transition zone in viscosity are shown in Fig. 9 for earth models L.1, L.4 and L.5. As for Fig. 6, results apply to a saw-tooth loading history (Fig. 5). However, the radius of the rectan-
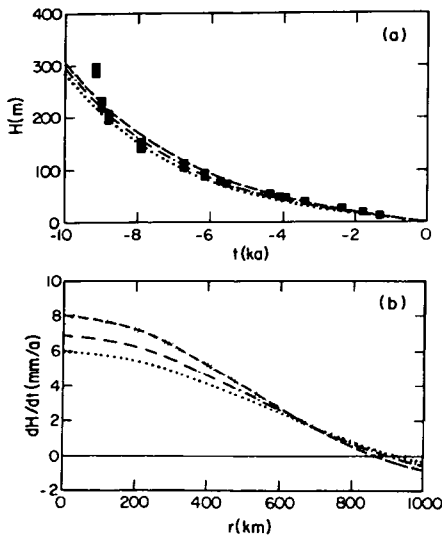
Fig. 10a and b. As for Fig. 4 except that predictions apply to load model 2 with $h_0^2/R = 3.0 \times 10^{-3}$ km and earth model L.5 (*dashed*), earth model L.4 (*dot-dashed*) or earth model L.1 with $h_1 = 200$ km (*dotted*); associated free-air gravity prediction at $r = 0$, $t = 0$ is $\Delta g = -10.9$ mgal (*dashed*), $\Delta g = -7.5$ mgal (*dot-dashed*) or $\Delta g = -3.5$ mgal (*dotted*)
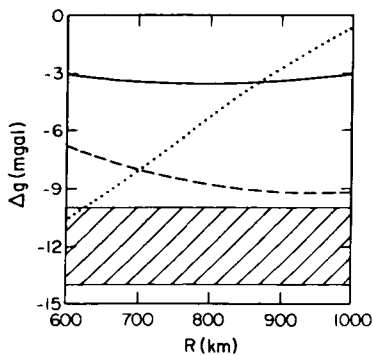

Fig. 11. Free-air gravity prediction Δg at $r = 0$, $t = 12$ ka as function of load radius R; predictions apply to saw-tooth loading history (Fig. 5) and earth model L.1 with $h_1 = 200$ km (*solid*), earth model M.4 with $h_1 = 200$ km, $\rho_3 - \rho_2 = 390$ kg m^{-3} and $\eta_3 = 2.0 \times 10^{21}$ Pa s (*dashed*) or earth model L.5 (*dotted*); *cross-hatched* band indicates glacial component of gravity anomaly (Fig. 1)

holds for free-air gravity. For earth model L.5, peak values of -11 mgal are predicted.

By intuitive reasoning, the importance of lithospheric relaxation is expected to depend on the ratio between load radius and lithospheric thickness. If this ratio is large, the lithosphere is virtually "transparent"; conditions close to local compensation apply, and the response should be insensitive to lithospheric relaxation.

This is illustrated in Fig. 11, which, for the saw-tooth loading history (Fig. 5), shows gravity predictions for rectangular loads of different radii. Comparison of the anomalies for earth models L.1 and L.5 shows that lithospheric relaxation becomes insignificant if the load radius exceeds about 700–800 km [see Wolf (1985a, Fig. 13) for a different example]. Loads of larger radii are, however, sensitive to lower-mantle viscosity and to internal buoyancy associated with the density contrast at 670 km depth, as shown for earth model M.4. For comparison, Fig. 11 also shows filtered peak gravity values according to Balling (1980) (without corrections for the long-wavelength geoid high).

Conclusion

The main conclusion of this study is that uplift data from Ångermanland and uplift-rate data from a profile in the Gulf of Bothnia are insufficient to constrain lithospheric thickness in Fennoscandia. The study has placed special emphasis on earth models with a lithosphere of about 200 km thickness and shown that these models are compatible with the two data sets. In a previous investigation, a lithosphere of about 70 km thickness was adopted, and a comparable fit of the data sets used here was achieved (Cathles, 1975, pp. 184–191).

A characteristic feature of interpretations that use earth models with a thin lithosphere appears to be that an asthenosphere is required below the lithosphere. Various model calculations have shown that the presence of an asthenosphere controls the movement of the zero-crossings separating the downwarped central region from the upwarped peripheral region. If mantle viscosity is uniform, the zero-crossings move inward after deglaciation. The presence of an asthenosphere leads, however, to stationary zero-crossings or even reverses the direction (e.g. Cathles, 1975, Figs. IV-28 and IV-29). At present, opinions differ on the movement of the zero-crossings in Fennoscandia (e.g. Cathles, 1980; Mörner, 1980). This feature therefore cannot be employed yet as circumstantial evidence for the thickness of the lithosphere.

More promising for this purpose are the develelled strandlines associated with pro- or post-glacial lakes or seas. If the strandlines are sufficiently old, their tilts are sensitive to lithospheric thickness. Pro-glacial-lake tilts were used to constrain lithospheric thickness in North America (Walcott, 1970; Wolf, 1985b, 1986). The interpretations favoured a thickness of less than 100 km, which is lower than Peltier's (1984) estimate of about 200 km based on relative sea-level data from the North American east coast. In Fennoscandia, a complete sequence of strandlines has been mapped and dated (e.g. Donner, 1980; Eronen, 1983). The oldest of these strandlines was formed at approximately 10 ka B.P. It is therefore pro-glacial, and its tilt is expected to be sensitive to lithospheric thickness. A careful analysis of strandline tilt may therefore help resolve the ambiguity in the interpretation.

gular load is reduced to 600 km. Because of the long relaxation times of the modes supported by the transition zone (Wolf, 1985a, Fig. 7), the initial decay of the excess deformation produced by the cyclic loading is not appreciable. Therefore, predictions of *relative* uplift are nearly unaffected. The *absolute* value of the surface depression at time $t = 12$ ka, and thus the theoretical free-air gravity anomaly, is, however, two- to threefold larger compared with the model without transition zone.

This is substantiated by Fig. 10, which shows uplift and uplift-rate predictions for the same earth models. The theoretical curves apply to load model 2. During load cycles 1–19, $R = 600$ km; during load cycle 20, $h_0^2/R = 3.0 \times 10^{-3}$ km. The fit is optimized for earth model L.5, but, as expected, theoretical uplift proves essentially insensitive to the viscosity stratification of the lithosphere. The opposite

The second aspect of this study has been the investigation of mechanisms which are capable of enhancing the gravity predictions without sacrificing the fit of the uplift data. Peltier and Wu (1982) achieved this largely by allowing sufficient internal buoyancy. The present study has restricted internal buoyancy to the density contrast at 670 km depth, in order to display more clearly the effect of lower-mantle viscosity on the gravity predictions. Alternatively, a transition zone in viscosity has been invoked to enhance the gravity anomaly. Either modification allows the prediction of negative anomalies of up to 11 mgal. This is rather small compared with the value proposed by Balling (1980) for the glacial component of the Fennoscandian gravity anomaly. Conversely, it is large in view of Anderson's (1984) study, which implies that the glacial component is minor.

Whether the Fennoscandian gravity data can constrain the earth's viscosity structure therefore depends on accurate determination of the size of the non-glacial component of the anomaly. Until this problem has been solved, studies of the kind discussed here mainly serve to demonstrate that interpretations using deep-flow models do not fail automatically if the glacial component turns out to be large.

References

Anderson, A.J.: Geophysical interpretation of features in the marine geoid of Fennoscandia. Mar. Geophys. Res. 7, 191–203, 1984

Balling, N.: The land uplift in Fennoscandia, gravity field anomalies and isostasy. In: Earth rheology, isostasy, and eustasy, N.-A. Mörner, ed.: pp. 297–321, New York: Wiley 1980

Bemmelen, R.W. van, Berlage, H.P. jr.: Versuch einer mathematischen Behandlung geotektonischer Bewegungen unter besonderer Berücksichtigung der Undationstheorie. Gerlands Beitr. Geophys. 43, 19–55, 1935

Cathles, L.M.: The viscosity of the earth's mantle. Princeton: Princeton University Press 1975

Cathles, L.M.: Interpretation of postglacial isostatic adjustment phenomena in terms of mantle rheology. In: Earth rheology, isostasy, and eustasy, N.-A. Mörner, ed.: pp. 11–43. New York: Wiley 1980

Clark, J.A., Farrell, W.E., Peltier, W.R.: Global changes in postglacial sea level: a numerical calculation. Quat. Res. 9, 265–287, 1978

Daly, R.A.: The changing world of the ice age. New Haven: Yale University Press 1934

De Geer, E.H.: Skandinaviens geokronologi. Geol. Fören. Stockholm Förh. 76, 299–329, 1954

Donner, J.: The determination and dating of synchronous Late Quaternary shorelines in Fennoscandia. In: Earth rheology, isostasy, and eustasy, N.-A. Mörner, ed.: pp. 285–293. New York: Wiley 1980

Dziewonski, A.M., Anderson, D.L.: Preliminary reference earth model. Phys. Earth Planet. Inter. 25, 297–356, 1981

Eronen, M.: Late Weichselian and Holocene shore displacement in Finland. In: Shorelines and isostasy, D.E. Smith, A.G. Dawson, eds.: pp. 183–207. New York: Academic Press 1983

Fairbridge, R.W.: Eustatic changes in sea level. In: Physics and chemistry of the earth, Vol. 4, L.H. Ahrens, F. Press, K. Rankama, S.K. Runcorn, eds.: pp. 99–185. London: Pergamon Press 1961

Farrell, W.E., Clark, J.A.: On postglacial sea level. Geophys. J.R. Astron. Soc. 46, 647–667, 1976

Gilbert, F., Dziewonski, A.M.: An application of normal mode theory to the retrieval of structural parameters and source mechanisms from seismic spectra. Philos. Trans. R. Soc. London Ser. A 278, 187–269, 1975

Haskell, N.A.: The motion of a viscous fluid under a surface load. Physics 6, 265–269, 1935

Imbrie, J., Imbrie, K.P.: Ice ages, solving the mystery. Hillside: Enslow 1979

Jordan, T.H.: Continents as a chemical boundary layer. Philos. Trans. R. Soc. London Ser. A 301, 359–373, 1981

Lidén, R.: Den senkvartära strandförskjutningens förlopp och kronologi i Ångermanland. Geol. Fören. Stockholm Förh. 60, 397–404, 1938

Lliboutry, L.A.: Rheological properties of the asthenosphere from Fennoscandian data. J. Geophys. Res. 76, 1433–1446, 1971

McConnell, R.K. jr.: Viscosity of the mantle from relaxation time spectra of isostatic adjustment. J. Geophys. Res. 73, 7089–7105, 1968

Mörner, N.-A.: The Fennoscandian uplift: geological data and their geodynamical implication. In: Earth rheology, isostasy, and eustasy, N.-A. Mörner, ed.: pp. 251–284. New York: Wiley 1980

Niskanen, E.: On the upheaval of land in Fennoscandia. Ann. Acad. Sci. Fenn. Ser. A 53, 1–30, 1939

Paterson, W.S.B.: The physics of glaciers, 2nd edn. Oxford: Pergamon Press 1981

Peltier, W.R.: The thickness of the continental lithosphere. J. Geophys. Res. 89, 11303–11316, 1984

Peltier, W.R., Andrews, J.T.: Glacial-isostatic adjustment, 1, the forward problem. Geophys. J.R. Astron. Soc. 46, 605–646, 1976

Peltier, W.R., Farrell, W.E., Clark, J.A.: Glacial isostasy and relative sea level: a global finite element model. Tectonophysics 50, 81–110, 1978

Peltier, W.R., Wu, P.: Mantle phase transitions and the free air gravity anomalies over Fennoscandia and Laurentia. Geophys. Res. Lett. 9, 731–734, 1982

Walcott, R.I.: Isostatic response to loading of the crust in Canada. Can. J. Earth Sci. 7, 716–727, 1970

Walcott, R.I.: Past sea levels, eustasy and deformation of the earth. Quat. Res. 2, 1–14, 1972

Walcott, R.I.: Structure of the earth from glacio-isostatic rebound. Annu. Rev. Earth Sci. 1, 15–37, 1973

Walcott, R.I.: Rheological models and observational data of glacio-isostatic rebound. In: Earth rheology, isostasy, and eustasy, N.-A. Mörner, ed.: pp. 3–10. New York: Wiley 1980

Wolf, D.: The relaxation of spherical and flat Maxwell earth models and effects due to the presence of the lithosphere. J. Geophys. 56, 24–33, 1984

Wolf, D.: The normal modes of a layered, incompressible Maxwell half-space. J. Geophys. 57, 106–117, 1985a

Wolf, D.: An improved estimate of lithospheric thickness based on a reinterpretation of tilt data from Pleistocene Lake Algonquin. Can. J. Earth Sci. 22, 768–773, 1985b

Wolf, D.: On deglaciation-induced perturbations of the geoid. Can. J. Earth Sci. 1986 (in press)

Wu, P., Peltier, W.R.: Glacial isostatic adjustment and the free air gravity anomaly as a constraint on deep mantle viscosity. Geophys. J.R. Astron. Soc. 74, 377–449, 1983